Monopile damage assessment from impact with a sub-sea boulder, using an LS-DYNA methodology

David McLennan[1], Francesca Palmieri[1], Andrew Cunningham[1], James Go[1], Richard Sturt[1], Paul Morrison[1], César Tejada[2], Georgios Perikleous[3], Jacob Brandt[3], Mikkel Lubek[4]

[1]Ove Arup & Partners Ltd, London, UK

[2]Ørsted A/S, London, UK

[3]Ørsted A/S, Copenhagen, DK

[4]Ørsted A/S, Skærbæk, DK

1 Abstract

During the installation of monopiles (MP) for the offshore wind turbine industry, there is a site-specific risk of impact with submerged sub-sea boulders, depending on the nature of the site geology. Factors such as boulder size, boulder depth, soil properties, and impact angle, will influence the level of damage experienced by the MP due to the boulder impact.

For assessing this damage, an LS-DYNA finite element (FE) methodology is demonstrated in this paper, with the MP modelled using thick shells, and the resistance provided by the soil modelled using discrete beams. For tubular MP geometry, the discrete beam approach has the advantage of reducing the analysis run-time by an order of at least 100x, compared to an approach which requires the modelling of a solid element mesh soil block (such as the established approach of a Coupled Eulerian-Lagrangian mesh). Material properties of the soil are obtained from real-world soil data, and characterised via closed-form solutions and supplementary FE analyses. The methodology makes use of a sequential introduction of soil elements and various contact definitions, to allow for a physically representative interaction between the MP and soil.

The analysis begins with the toe of the MP about to make contact with the boulder, and ends at the final MP embedment depth, having interacted with the boulder for the duration of the remaining portion of the installation sequence. A real-world MP installation involves thousands of individual hammer impacts, but in this study the MP is pushed downwards with a constant velocity throughout the analysis. This modelling simplification has been justified via sensitivity studies, and is another technique which considerably reduces analysis runtime, compared to the alternative of modelling each individual hammer impact of the installation sequence. It results in a 10-metre push having an analysis runtime of approximately 3 hours on 32 CPU.

Results from this LS-DYNA methodology are obtained for a representative range of site-specific input parameters. These results are used to influence on-site MP installation strategies, to avoid locations with known boulders above a certain size, and hence reduce the risk of MP damage and refusal.

2 Introduction

The construction of offshore wind turbine foundations can take many forms: some are floating structures, and some are driven monopile (MP) foundations which embed deep into the seabed – this paper focuses on the latter, for a generic tubular MP design. The seabed's local geology is a governing factor in whether the MP foundation will be installed successfully. The general stratigraphy of the area can be accurately assessed using geophysical investigations, borehole drilling and in-situ testing, however the presence of subsea boulders (such as in former glacial regions of the world) can pose a bigger challenge due to the uncertainty of their exact locations and material properties. Impact with a large, tough boulder during MP installation in a stiff geotechnical stratum can lead to a damaged MP, or refusal of the MP to embed any further (see *Fig.1*). This extrapolates to unforeseen complications with forcing the MP to fully embed, and a potential abandoned installation, with the associated waste in time, material costs, and energy expended on the installation up to that point. It is therefore of great value to understand the likely boulder sizes, distributions, and risk of MP damage in the event of an impact, before attempting the on-site installation of these wind turbine foundations.

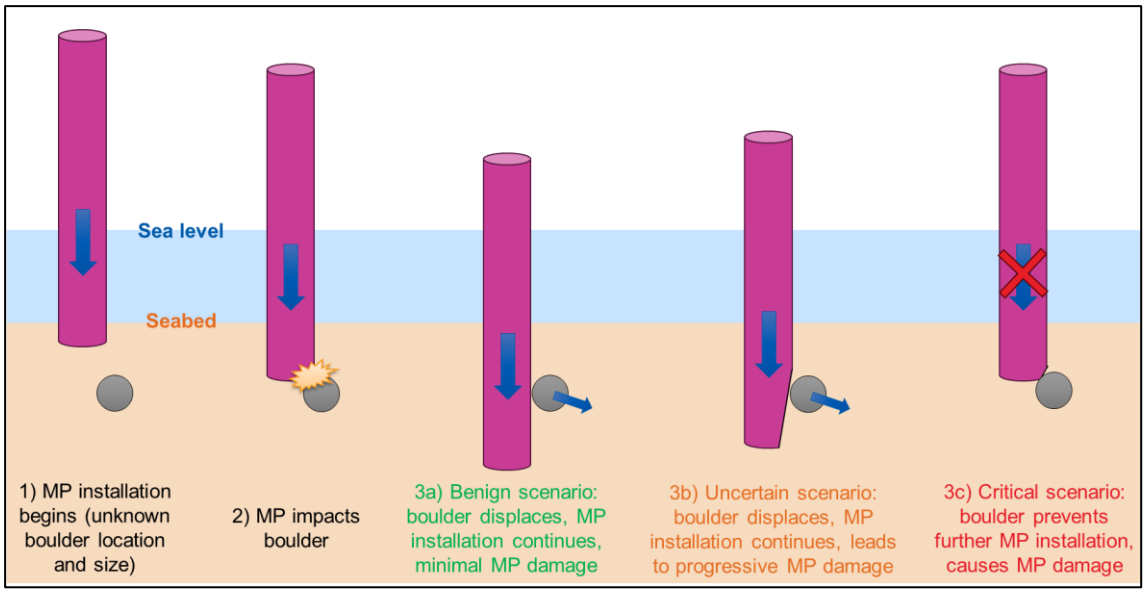

Fig.1: Illustration of the MP installation process, and potential consequences of boulder impact.

There are advantages to an efficient LS-DYNA methodology for predicting the level of damage on a steel MP in the event of subsea boulder impact, and how this damage would be expected to vary across a range of likely site conditions. This paper demonstrates this methodology in principle.

3 LS-DYNA model

The geometry, mesh, element types, and prescribed motion for the LS-DYNA model are shown in *Fig.2*. The analysis modelled a constant velocity push for the entire MP, using **`*INITIAL_VELOCITY`** and **`*BOUNDARY_PRESCRIBED_MOTION`** definitions. It was shown that MP damage was not sensitive to the velocity magnitude in the range of 1 to 10m/s, therefore 10m/s was chosen – fast enough for an efficient analysis runtime, and to be compatible with the mesh resolution.

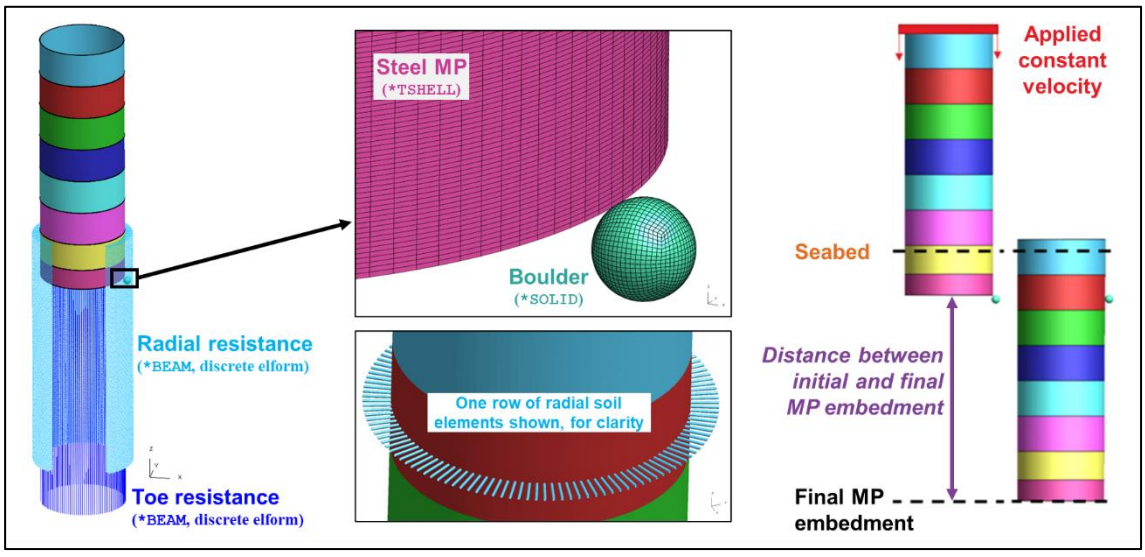

Fig.2: The geometry, mesh, element formulations, and constant velocity prescribed motion used within the LS-DYNA model, with initial and final positions of the MP shown relative to the boulder.

3.1 Monopile model

The MP geometry was that of a hollow tube, consisting of sections of rolled steel (known as “cans”), each can with a different wall thickness, welded one above the other. An efficiency was achieved by

modelling only the lower half of the MP (a total of eight cans), as depicted in *Fig.2*. The top of the modelled MP always remained above the level of the seabed, until the point of final embedment. The bottom can on the MP is known as the “driving shoe” – it has the largest wall thickness to help prevent MP distortion during driving, which has been shown to occur when a driving shoe was not included [1]. Inclusion of the top half of the MP was shown not to significantly change the installation behaviour or damage incurred due to boulder impact, so the extent of MP modelled was restricted to the height required to ensure that the MP remained in full contact with soil until final embedment.

The LS-DYNA model used fully integrated, selectively reduced thick shell elements, defined by four nodes on the outer surface of the MP and four nodes on the inner surface. These thick shells were defined to have a total of 20 integration points per element, and 128 elements around the circumference of the MP. Elastoplastic material properties were defined with a stress-strain curve representing steel grade S355. Strain-rate dependency of the steel was included using the Cowper-Symonds approach from DNV-RP-C208 [2].

3.2 Soil modelling

For soil penetration problems, it is common to model the soil domain using a large number of solid elements, typically with a Coupled Eulerian-Lagrangian (ALE) mesh [3]. Instead, the methodology described in this paper used a series of non-linear discrete beams to capture the resistance of the soil to the moving MP, without needing to model the soil in detail. This approach was far less computationally expensive than a solid element soil block approach and provided a reasonable representation of the vertical variation in soil resistance. Comparisons between element count and analysis runtime are given in Section 5.2.

The modelling method used for this paper relied on properties of the beam elements that offer a reasonable approximation of the soil’s resistance against the moving MP. The toe resistance of the soil was derived from site-specific measurements, processed using a method by Alm & Hamre [4]. These material properties were assigned to the corresponding discrete beam elements, with one node connected at the base of the MP, equally spaced all around the MP’s circumference, and the other node fully fixed at a depth greater than the final embedment depth of the MP. Each toe resistance beam was given an identical force/displacement behaviour curve, with greater resistance being offered at greater depth, as shown in the right-hand graph of *Fig.3*.

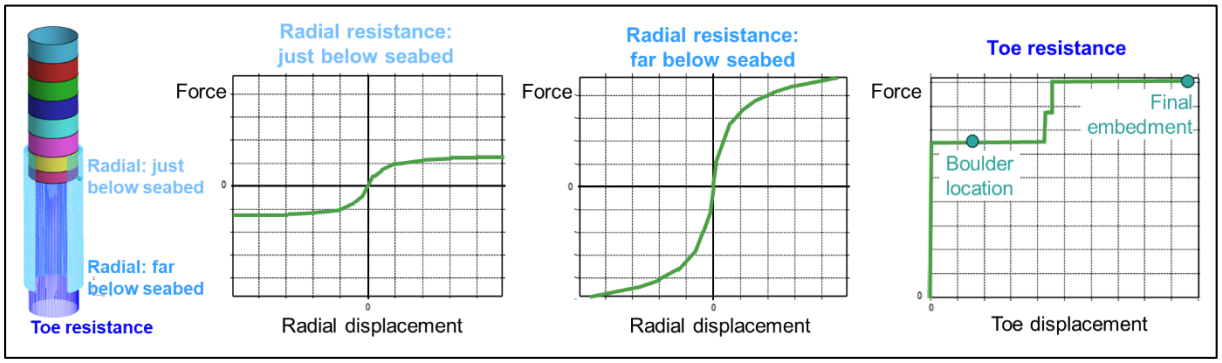

Fig.3: Radial resistance modelling, including variation across two locations up the height of the MP, plus toe resistance modelling, both showing increased resistance with depth.

The radial resistance of the soil was derived from site-specific measurements, in combination with an LS-DYNA model in which a small region of MP and soil were modelled by solid elements, and the hysteretic properties characterised using a method by Darendeli [5]. These material properties were assigned to the corresponding discrete beam elements around the outer circumference of the MP in the LS-DYNA model. The variation in radial resistance with depth was captured by having different material cards (defining the loading and unloading behaviour) for soil elements at different heights – two examples are shown in *Fig.3* (the unloading behaviour is not shown). These radial soil elements were modelled on the outside of the MP only (i.e., there were no soil elements inside the MP) due to their material behaviour curve being defined to act in both directions (i.e., positive or negative radial displacement). The outer node of each radial soil element was fully fixed in space, with the inner node

being in contact with the MP. Friction was defined on the contact to resist sliding of the MP through the soil.

A key challenge was setting the initial radial position for each discrete beam element (corresponding to the "origin" of the beam's force/displacement curve). This gets determined by the radial position at which the MP toe cuts through the soil, which is not known in advance and varies at different depths and at different angular positions around the MP's circumference, depending on the deformations of the MP toe that have occurred before it reaches that specific depth. An innovative method involving **`*CONTROL_STAGED_CONSTRUCTION`** was adopted to generate new discrete beams during the analysis, as the MP moved downwards. A new row of soil elements got generated at the time at which the MP toe reached the depth of that row. Forces in the soil elements were calculated based on the radial displacement relative to the element length at the time of generation. Thus, any prior deformation of the MP surface (such as localised distortion due to impact with the boulder) was locked in by the newly generated soil elements. This approach is illustrated in *Fig.4* and *Fig.5*.

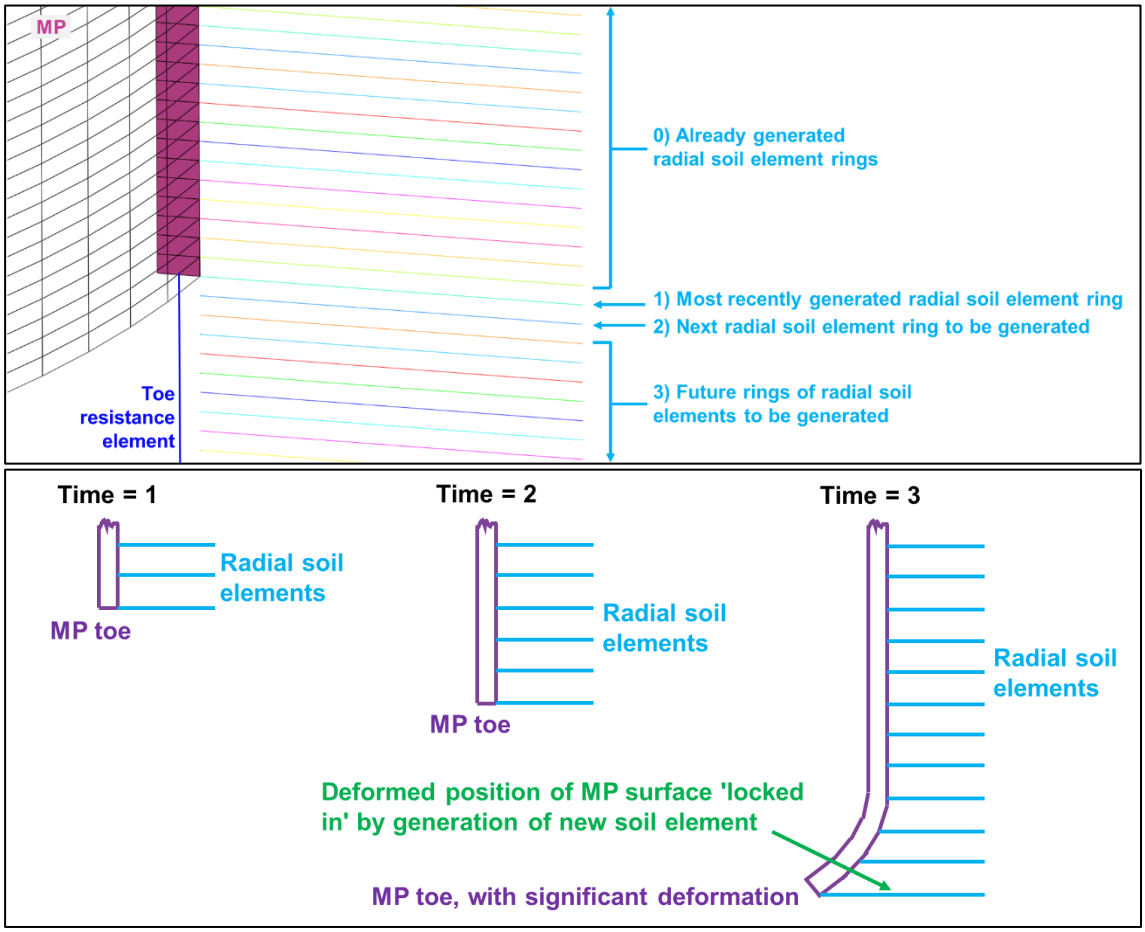

Fig.4: The generation of soil resistance elements, noting that the node positioning of each new soil element depends on the current position of the toe of the MP.

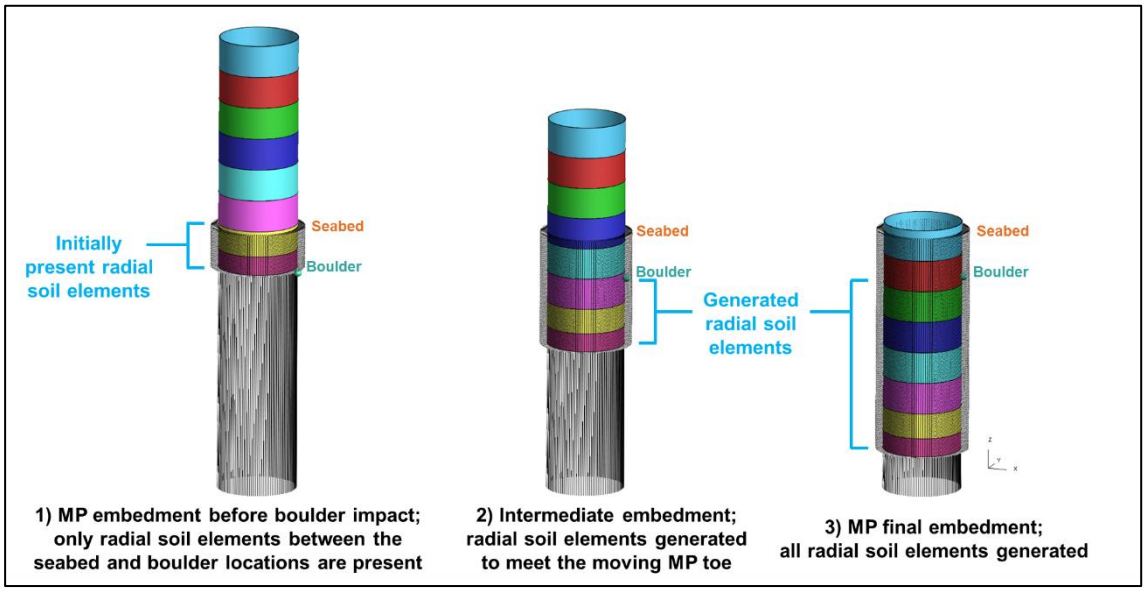

Fig.5: The time-dependent generation of radial soil resistance elements during the LS-DYNA analysis, from initial embedment (prior to boulder impact) to final embedment of the MP.

The modelling of the resistance of the soil surrounding the boulder adopted a similar approach, shown in *Fig.6*. The boulder was resisted from translating and rotating via spring and damper elements with properties derived from site-specific measurements and analytical solutions.

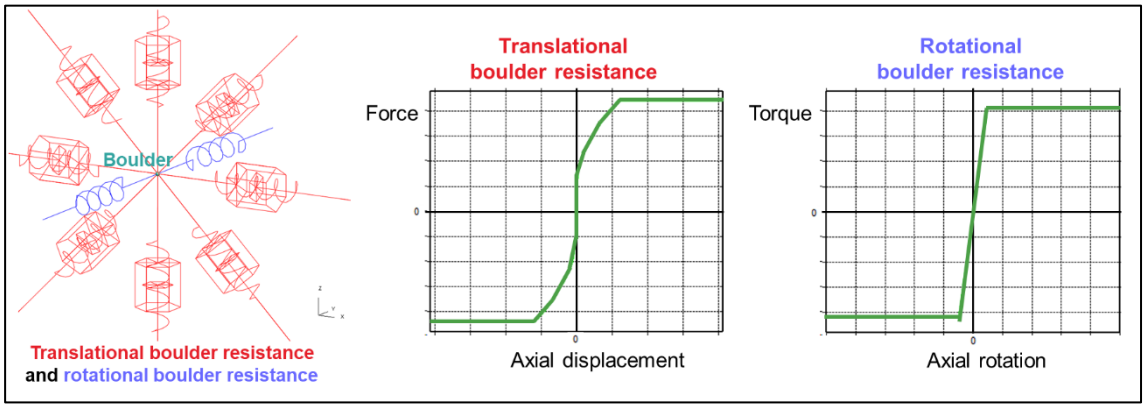

Fig.6: Modelling of resistance of the soil surrounding the boulder via spring and damper elements, including loading curves for the translational and rotational resistance.

The boulder itself was modelled using fully integrated solid elements, with eight integration points per element. A spherical shape was chosen for the purpose of this paper. A wide range of boulder shapes and compositions will exist on a given site, giving a range of different responses from MP impact. The possibility of the MP impact causing cracking or splitting of the boulder was not modelled here – such effects would be expected to reduce the resistance and damage caused by the boulder.

3.3 Oasys PRIMER JavaScripts

A series of Oasys PRIMER JavaScripts were developed to quickly generate the MP mesh, the surrounding arrays of radial and toe resistance elements, their associated **`*SECTION`** and **`*MATERIAL`** cards, and the staged introduction of the radial soil resistance elements. The scripts have the flexibility to produce a thin shell or thick shell MP, for any MP height, with any number of cans; each can with whatever height, wall thickness, and diameter that the MP design dictates. This reduced the model creation timeline down from several days to only a few minutes – requiring only the creation of a CSV file to contain the geometric input parameters, and for computing the JavaScripts within PRIMER.

4 LS-DYNA analyses

To achieve the objective of understanding a likely range of MP behaviours during installation for a specific MP installation site, parametric studies across some key variables were performed, with those variables shown in *Table 1* and *Fig.7*. The specific values of each variable would need to be decided differently for each site, based on known data for that site.

These variables reduced to a total of ten LS-DYNA analyses (listed with details in *Table 3*). The variation in impact angle was only computed on the medium boulder size in UB soil – the level of damage on the MP from impact with the large boulder size was deemed too great, so the on-site strategy would be to avoid installation of MPs in specific locations where large boulders are observed in the survey data.

Variable	**Values**
Soil material properties	Upper Bound (UB), Lower Bound (LB)
Boulder location (depth)	Shallow, Deep
Boulder diameter	Medium, Large
MP/boulder impact angle	45º, 75º, 90º

Table 1: The key variables for these LS-DYNA analyses.

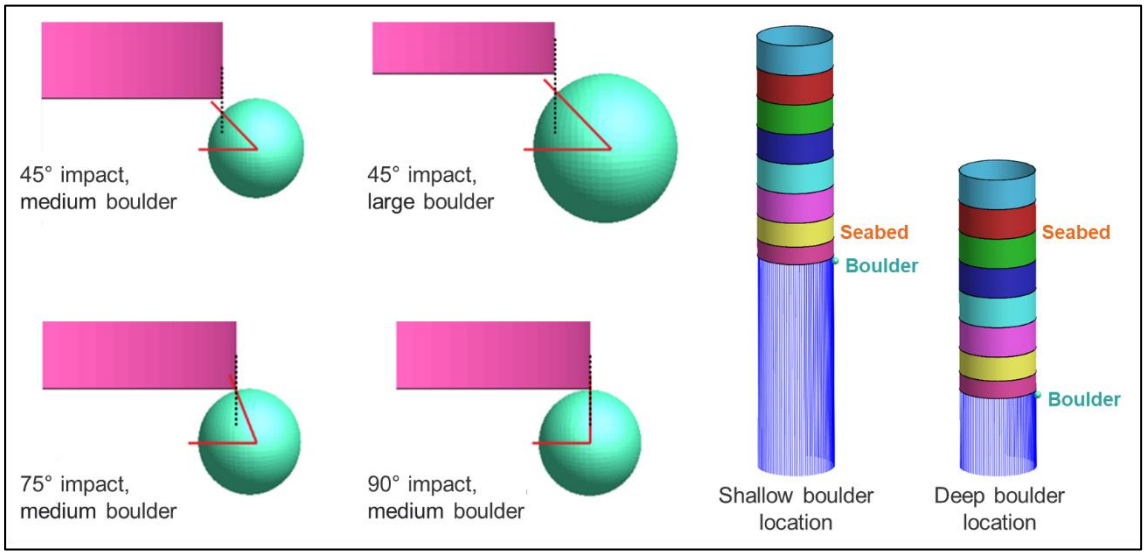

Fig.7: Illustration of the key variables from Table 1, for these LS-DYNA analyses.

5 LS-DYNA results

The primary objective for these analyses is to detect the conditions (i.e., combinations of input parameters) necessary for the type of deformation shown in *Fig.5:,* whereby a small initial indentation at the MP toe becomes magnified during subsequent driving. In extreme cases, deformations can become so large that the MP cannot be driven any further (i.e., refusal). A secondary objective is to predict plastic deformations in regions of the MP that may be vulnerable to fatigue damage caused by wind and wave loading during the wind turbine's service life.

5.1 Sensitivity to input variables

The sensitivity of this MP to the variables listed in *Table 1* was assessed via the metrics and figures summarised in *Table 2*, with a description of the results also provided. As measures of MP deformation, the change in MP diameter was recorded (in both X and Y radial directions, defined in *Fig.9*), along with any plastic strain occurring in the MP. The force time history within the MP was also recorded and compared with the peak force from a single hammer impact. Note that the results presented here are a snapshot of one arbitrary site, and general trends seen here may not be applicable to other sites.

For an assessment of the potential for MP refusal during installation, it is observed that all simulations successfully allowed the MP to displace to its final embedment depth, without buckling of the MP wall, or large areas of plastic failure. It is therefore concluded that the risk of MP refusal during installation is low, for the range of soil conditions and boulder sizes considered.

It can be observed from *Fig.8, Fig.9*, and *Fig.10*, that a significant advantage of this methodology is the ability to track the structural changes in the MP over time during the entire MP installation process. This can be observed via looking at the changing profile of the MP distortion, specifically the tendency of the indentation to either stabilise or increase after the boulder impact, and associated stress and strain time histories for elements within the MP.

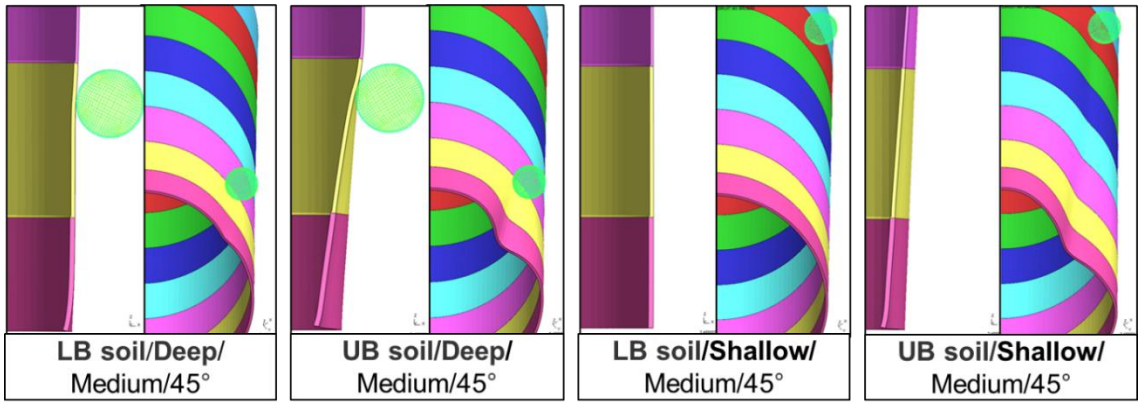

Fig.8: Comparison of MP deformation (unmagnified), for a range of input conditions.

Variable	**Assessment metric**	**Description of results**
Soil material properties	Change in MP diameter *(Fig.8, Fig.9)* Plastic strain in the MP (*Fig.10*)	Up to 9x larger MP toe distortion in the UB soil, compared to LB soil, and larger peak plastic strains at the impact point. LB soil gave a stabilising effect to the MP distortion (shown by the curve plateau), whereas the UB soil caused the MP to continue with increasing distortion, right up to the MP's final embedment depth.
Boulder location (depth)	Change in MP diameter *(Fig.8, Fig.9)* Plastic strain in the MP (*Fig.10*)	Typically, larger MP toe distortion (except for the large diameter/UB soil scenario) and larger peak plastic strains for the deep boulder location, compared to shallow.
Boulder diameter	Change in MP diameter (*Fig.9*) Plastic strain in the MP (*Fig.10*)	Between 3x and 6x larger MP toe distortion for the large boulder diameter, compared to the medium diameter, and larger peak plastic strains at the impact point.
MP/boulder impact angle	Change in MP diameter (visible in *Fig.10*) Plastic strain in the MP (*Fig.10*)	The 75^{o} impact angle generated largest plastic strains. The 90^{o} impact prevented the boulder from moving to one side, resulting in the MP pushing the boulder downwards to its final embedment depth, and gave the largest resistive force against driving.

Table 2: Assessment metrics (and corresponding figures in this paper) for each variable of sensitivity.

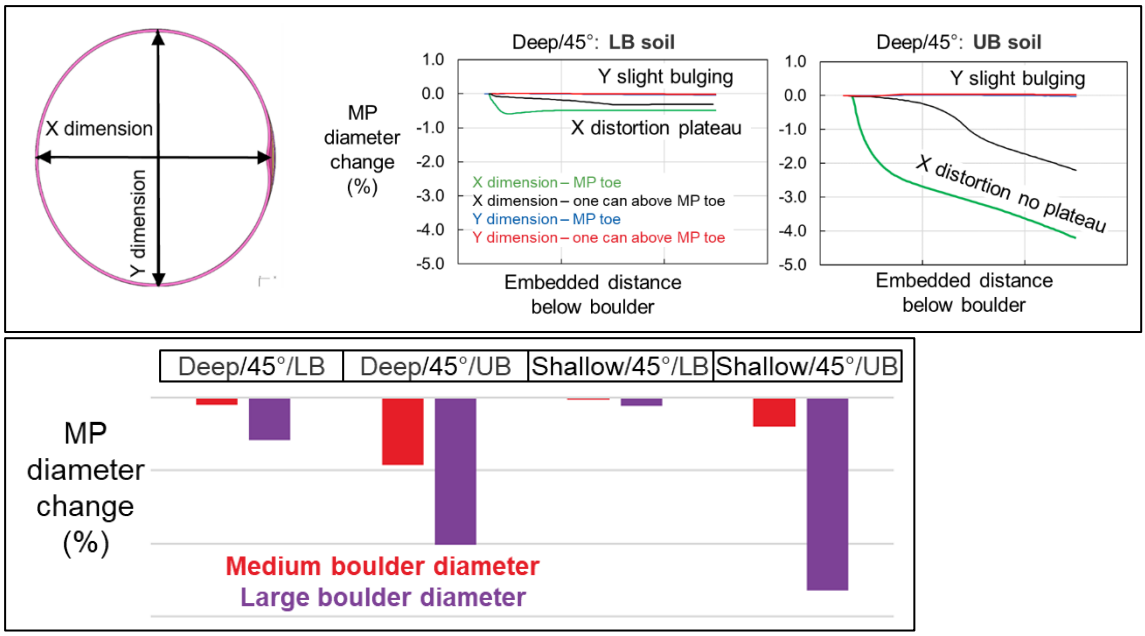

Fig.9: Comparison of the change in MP diameter after impact, for a range of input conditions.

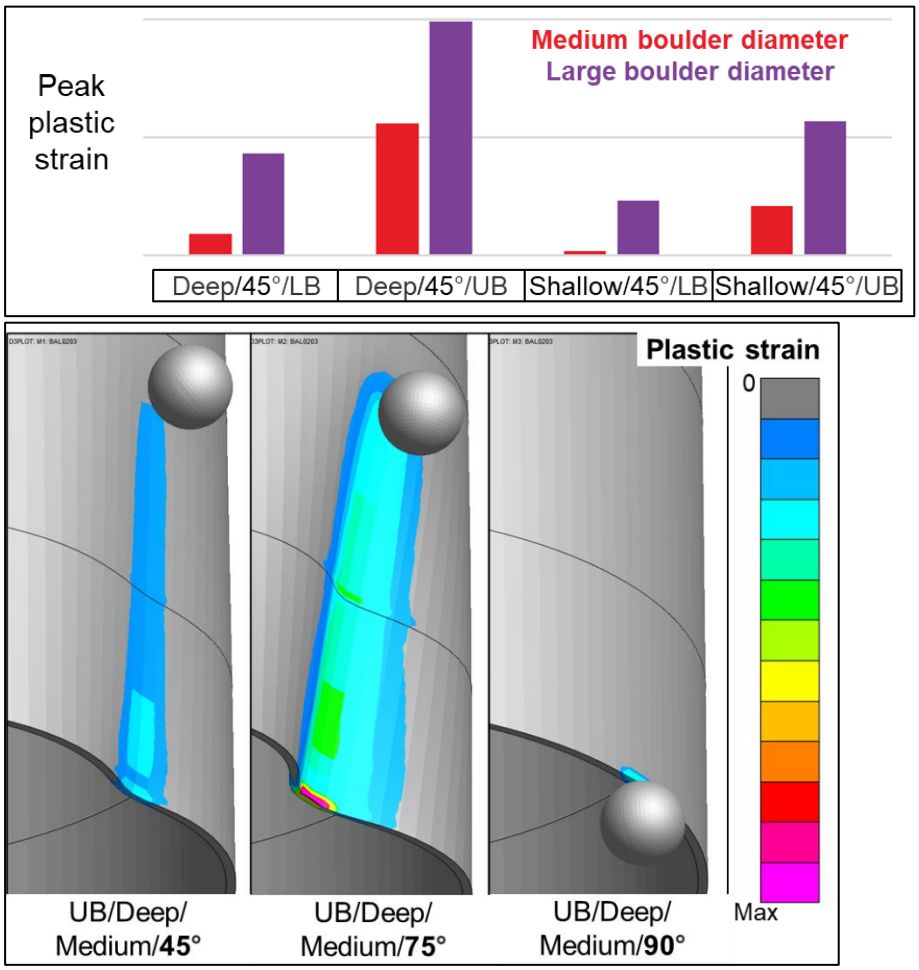

Fig.10: Comparison of plastic strain in the MP, for a range of input conditions.

5.2 Analysis runtime

For comparing this methodology to alternative approaches, a key performance metric is analysis runtime. For the ten analyses performed for this paper, total analysis runtime is reported in *Table 3*, also normalised on a "per 1 metre of MP driving" basis. All analyses were performed on a high-performance computing cluster, across 32 CPU. Note that the four "shallow depth" boulder analyses took longer to compute "per 1 metre of MP driving", most likely due to the larger contacted area between the MP and boulder which developed during the analysis, and subsequent larger region of MP element distortion.

Analysis description	**Total analysis runtime**	**Analysis runtime per 1 metre of MP driving**
Shallow/Medium boulder (LB/UB, 45^{o})	~13h 20m	~27 minutes
Deep/Medium boulder (LB/UB, 45/75/90^{o})	~2h 50m	~17 minutes
Shallow/Large boulder (LB/UB, 45^{o})	~13h 40m	~28 minutes
Deep/Large boulder (LB/UB, 45^{o})	~3h 0m	~18 minutes

Table 3: Comparison of analysis runtimes for all analyses computed for this paper (all using 32 CPU).

An approximate count for the number of elements in the LS-DYNA model used for this paper is shown in *Table 4*. Alongside this is an estimate for the corresponding values in an equivalent solid soil block model capable of capturing the radial and toe resistances via an ALE approach. Note that tubular geometry (such as this MP) is particularly awkward for a solid element soil mesh due to the vastly different length scales between the thin MP wall (requiring detailed mesh refinement in this region if toe resistance is to be captured accurately), and the overall diameter of the MP.

The element count for the "equivalent solid soil block model" in *Table 4* assumes a tube-shaped region of soil mesh refinement for a distance of two wall thicknesses inside and outside the MP, with element length equal to 20% of MP wall thickness (as sketched in *Fig.11*), extending down to an embedment depth of 40 metres. A less refined region of solid elements beyond the MP would also be needed to ensure that the overall dimensions of the soil domain are large enough to avoid boundary effects from artificially constraining the model. This level of mesh density for a solid soil block model could result in an approximately ~500x increase to the number of elements in the model (*Table 4*), and approximately the same order of magnitude increase in analysis runtime, rendering the analysis unfeasible within typical project timeframes.

It may also be possible to model the soil with fewer, larger solid elements in an approach that does not attempt to capture toe resistance accurately; however, the number of elements required would still greatly exceed the number used by the approach proposed in this paper, even if the loss of accuracy of the toe resistance could be solved efficiently.

Soil modelling method	**Beams**	**Thick shells**	**Solids**
Discrete beam approach (used in this paper)	150,000	80,000	16,000
An equivalent solid soil block model	0	80,000	80-150 million

Table 4: The approximate counts of elements for the LS-DYNA approach used in this paper, compared to those of an equivalent solid soil block model with the mesh shown in Fig.11.

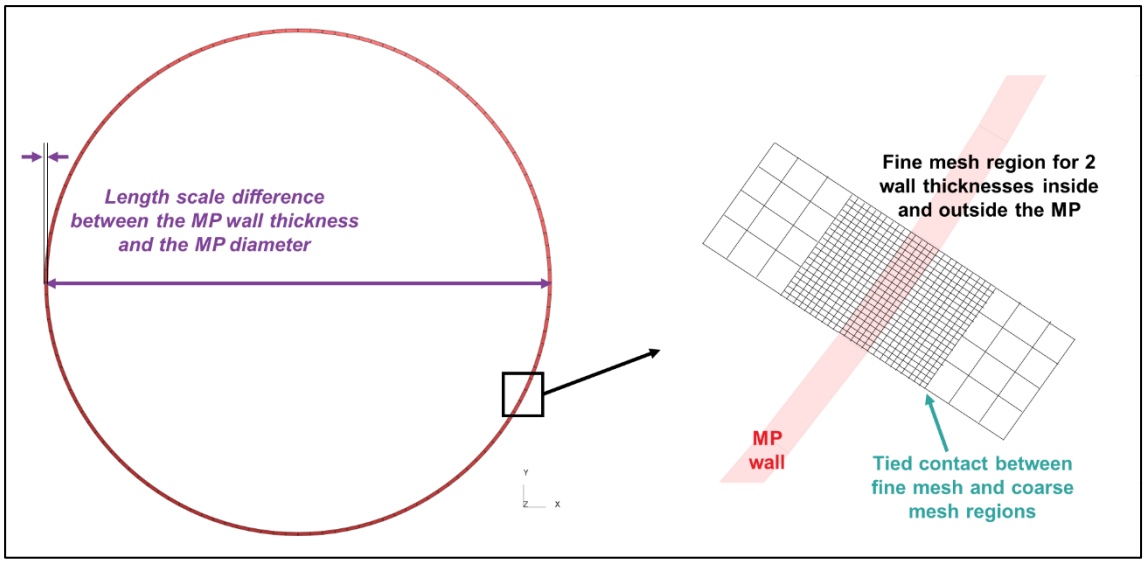

Fig.11: An example of the solid element mesh refinement required around the wall of a tubular MP for a solid element soil block model.

5.3 Further analysis related to MP installation

No quantitative validation of MP deformation was obtained for this paper, whilst noting that this would be a useful exercise. It is difficult to obtain accurate data for MP deformation behaviour in subsea locations during a real MP installation programme, so there is a need for experimental testing on scale models for comparison with an equivalent FE model.

The results of these LS-DYNA constant velocity push analyses are often complemented with results of LS-DYNA hammer impact analyses [6]. By explicitly modelling the hammer and applying the energy of a single hammer impact on to the top of the full-height MP, a good prediction of the downward MP displacement from a single hammer impact can be obtained, for any given embedment depth of the MP (noting that MP displacement will vary depending on the current embedment depth of the MP into the seabed). Other metrics such as element stresses, and the propagation and reflection of stress waves due to hammer impact can be observed from this type of analysis.

Magnitudes of MP displacement from a single hammer impact should align well between the LS-DYNA methodology, a GRLWEAP (geotechnic software) simplified methodology, and the values expected on site by experienced MP installation operators.

Further LS-DYNA analyses can also be conducted to provide the necessary design insights into the fatigue performance of the MP during installation, specifically for regions likely to experience stress concentrations such as at the welds between MP cans, at welded attachments (such as ladder mounting points, structural stiffeners) and at openings in the MP wall.

6 Conclusions

The LS-DYNA modelling methodology discussed in this paper is an effective way of assessing the potential for tubular MP damage during installation, including damage that develops progressively after a relatively small indentation by a boulder. It is important that MP damage is sufficiently small to avoid driveability issues, with the critical scenario being complete refusal of the MP to drive during installation. Although the analysis examples above do not explicitly show the refusal condition, the modelling method can predict the onset of large deformations that would lead to refusal.

The key metric of MP damage considered in this paper was the change of diameter (which varies with height), serving as a proxy for MP structural damage, and hence for increased risk of refusal to drive the MP deeper into the subsea strata. Additionally, plastic strain associated with the deformation, specifically at the weld locations between MP cans, was used to inform future fatigue performance

related to cyclic loading from wind and wave events. Peak forces within the MP from the push analyses can be compared to those from a single hammer impact.

The proposed modelling approach enables a turn-around time of a few hours, including model set-up and LS-DYNA computation. Contributors to the efficiency of the process are:

- Soil resistance modelled by discrete beam elements, leading to much-reduced element count (and hence analysis runtime) compared to a solid element soil mesh.
- Using a constant velocity prescribed motion (as an analogy to the true installation method of many thousand hammer impacts), with the specified velocity being as large as possible for computational efficiency without being so large as to give physically unreasonable results.
- Bespoke Oasys PRIMER JavaScripts, to reduce model set-up time from days to hours.

Thanks to the short turn-around time, the proposed modelling approach offers significant benefits:

- The ability to simulate the full MP installation process, from seabed to final embedment depth.
- The ability to observe the change in diameter and build-up of stresses and strains in the MP over time, caused by the MP moving into different strata of soil, and from boulder impacts.
- The ability to conduct parametric studies, for example on soil properties and boulder sizes and locations.
- The ability to compute results for different wall thicknesses of the MP's driving shoe, to assess how this important dimension would affect driveability.

The analyses illustrated in this paper help to inform site-specific MP installation strategies for offshore wind turbine designers and predict the total number of hammer impacts required to drive the MP to its final embedment depth. A typical final embedment depth would require the toe of the MP to be between 3 to 5 MP-diameters below the seabed, typically involving several thousand hammer impacts. If the installation occurs with minimal damage to the MP, then it will lower the risk of adverse effects on the MP's performance during the wind turbine's operational lifespan. The variability of soil and boulder conditions at one site, and across multiple sites, will mean that a successful MP design at one location may not be successful at another location, so this methodology should be adopted for each site individually.

7 Literature

[1] G. Musso, E. Nicolini, "Numerical study of flint/boulder behaviour during pile driving", Collegio di Ingegneria Civile, Politecnico di Torino, 2018.

[2] DNV-RP-C208, "Determination of structural capacity by non-linear finite element analysis methods", DNV, 2016.

[3] J. Nietiedt, M. Randolph, J. Doherty, C. Gaudin, "Numerical assessment of tip damage during pile installation in boulder-rich soils", Geotechnique, ahead of print, published online 14 July 2022.

[4] T. Alm, L. Hamre, "Soil Model for Pile Driveability Predictions Based on CPT Interpretations", Proceedings of the 15th International Conference on Soil Mechanics and Foundation Engineering, Istanbul, 2001, Vol. 2, pp. 1297–1302.

[5] M.B. Darendeli, "Development of a new family of normalized modulus reduction and material damping curves", The University of Texas at Austin, 2001.

[6] F. Palmieri, D. McLennan, F. Ciruela-Ochoa, A. Cunningham, J. Go, P. Morrison, C. Tejada, G. Perikleous, J. Brandt, M. Lubek, "Three-dimensional finite element modelling to assess the damage due to boulder impact during pile installation", Proceedings of the 10th European Conference on Numerical Methods in Geotechnical Engineering, 2023.